Nonisothermal Cure Kinetics in the Synthesis of Polybenzoxazine–Clay Nanocomposites

Zixing Shi,[1,2] Dingsheng Yu,[1] Yizhong Wang,[1] Riwei Xu[1]

[1]*School of Materials Science and Engineering, Beijing University of Chemical Technology, Beijing 100029, People's Republic of China*
[2]*School of Chemistry & Chemical Technology, Shanghai Jiao Tong University, Shanghai 200240, People's Republic of China*

Received 24 October 2001; accepted 4 June 2002

ABSTRACT: The ability to understand and model the mechanism of cure kinetics accurately is crucial for the production of thermosetting resin-based nanocomposites. This article reports on work performed to elucidate an accurate model of cure kinetics for the formation of polybenzoxazine–montorillonite nanocomposites through the use of differential scanning calorimetry with nonisothermal methods, including single-heating and multiple-heating methods. The results indicated that both the Kissinger and Ozawa methods for calculating the activation energy gave fairly close results of 115 and 120 kJ/mol, respectively. The reaction order was about 1.31, calculated from the single-heating method based on the autocatalytic method, and a comparison was made of the dynamic curing behaviors in the syntheses of polybenzoxazine and polybenzoxazine–montorillonite nanocomposites. © 2003 Wiley Periodicals, Inc. J Appl Polym Sci 88: 194–200, 2003

Key words: curing of polymers; nanocomposites; kinetics (polym.)

INTRODUCTION

The research of organic–inorganic nanocomposites is a stimulating fundamental field because they frequently exhibit unexpected hybrid properties synergistically derived from two components that are dramatically different from their bulk counterparts.[1] Some of the most promising composite systems are nanocomposites based on organic polymers and inorganic clay minerals consisting of layered silicates.[1] These polymer-layered silicate nanocomposites can exhibit increased modulus, decreased thermal expansion coefficients, reduced gas permeability, increased solvent resistance, and enhanced ionic conductivity with respect to the polymers alone.[2]

Montmorillonite (MMT) has been particularly important in forming effective polymer nanocomposites because of the intercalation chemistry. MMT is a crystalline, 2/1 layered clay mineral in which a central alumina octahedral sheet is sandwiched between two silica tetrahedral sheets.[3] Usually, MMT clays are modified by an onium ion substitution reaction with surface sodium ions; this renders the normally hydrophobic silicate surface organophilic and, therefore, enables the insertion of organic materials, including many polymers.[4]

Nanocomposites based on many polymers of different polarities, including polystyrene,[5] polycaprolactone,[6] poly(ethylene oxide),[7] polyamide,[4] polyimide,[8,9] epoxy,[3,10–12] polysiloxane,[13] and polyurethane,[14] have been successfully synthesized. However, there are only a few reports[15–19] on the synthesis of novel nanocomposites based on polybenzoxazines (PBZs).

PBZs constitute a novel class of phenolic resins that are formed from low molecular weight monomers by ring-opening polymerization without the evolution of byproducts.[20–25] They combine the thermal properties and flame retardance of phenolic resins with the excellent mechanical performance and molecular design flexibility of epoxy resins.[20–25] Inherently nonflammable PBZ resins exhibit high char yields, superior mechanical properties, and excellent processability through their flexible molecular design without sacrificing the advantages of conventional phenolic resins.[20–25]

We have found that the cure mechanism and kinetics in the synthesis of PBZ–MMT nanocomposites are quite different from those in the synthesis of pure PBZs.[26] The catalytic effect of the MMT surface on the ring-opening polymerization and the barrier effect of the silicate layers in the nanocomposites may account for this phenomenon.[3,27]

It has been clarified that during the production of composites based on thermosetting resins, the ability

Correspondence to: D. Yu (yuds@mailserv.buct.edu.cn).
Contract grant sponsor: Committee of the Natural Science Foundation of China; contract grant number: 59973003.

Journal of Applied Polymer Science, Vol. 88, 194–200 (2003)

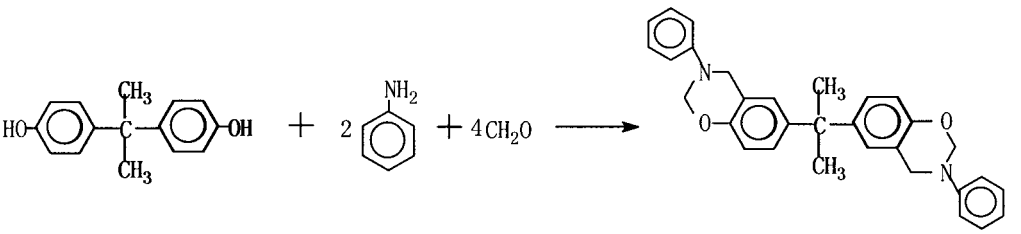

Scheme 1

to maximize the glass-transition temperature in the shortest possible time is crucial, as the transition temperature directly correlates to the highest possible service temperature without adverse effects.[27] Basic to such an optimal curing process is the need to first understand the physical curing mechanism and cure kinetics underlying the process and then to be able to model the cure process accurately.[27] Therefore, it is fundamentally necessary to research the cure mechanism and cure kinetic in the synthesis of PBZ–MMT nanocomposites so that we can establish the appropriate optimal curing process for producing nanocomposites with excellent properties. However, a comprehensive understanding of the mechanism and kinetics of cure has yet to be clearly established. Therefore, we investigated the cure kinetics of PBZ–MMT nanocomposites with differential scanning calorimetry (DSC) under a nonisothermal mode. This work is part of a larger study of the curing characteristics of PBZ–MMT nanocomposites. This particular part is concerned with an accurate description of the kinetics of cure with the information provided by DSC under a nonisothermal mode.

EXPERIMENTAL

Materials

Sodium montmorillonite (Na-MMT) was supplied by the Institute of Chemical Metallurgy of the Chinese Academy of Sciences (Beijing, China). Bisphenol, 37% aqueous formalin, aniline, and toluene were all analytically pure and were supplied by Beijing Chemical Reagent Co. (China).

Preparation of organically modified layered montmorillonite (O-MMT)

A dispersion of 30 g of Na-MMT in 6×10^{-4} m^3 of distilled water was added to a heated (80°C) solution of 26.02 g of celtyltrimethyl ammonium bromide $[C_{16}H_{33}(CH_3)_3N^+Br^-]$ in 10^{-4} m^3 of distilled water. The mixture was agitated vigorously for 1 h. With filtration, a precipitate was obtained. It was repeatedly washed with hot water and ethanol until no Br^- was detected in the filtrate by silver nitrate. The organotreated MMT was finally dried at 40°C *in vacuo*.

Preparation of the PBZ monomer bis(3-phenyl-3,4-dihydro-2H-1,3-benzoxazinyl) isopropane (BZ)

BZ was prepared from aniline, formaldehyde, and bisphenol by methods described in a previous article[20] and shown in Scheme 1.

Preparation of the PBZ monomer-solvated MMT (BZ–MMT) system

BZ (20 g) and 2 g of O-MMT were mixed together in 2×10^{-4} m^3 of toluene. The dispersion was stirred rigorously at 25°C for 10 h, and a well-dispersed mixture was obtained; then, a vacuum was employed for the removal of toluene.

Preparation of the PBZ–MMT nanocomposite samples for X-ray diffraction (XRD)

Sample were obtained by the heating of the mixture at 120°C for 2 h, at 160°C for 3 h, at 180°C for 2 h, and at 200°C for 1 h.

Structural characterization of the PBZ–MMT nanocomposites

X-ray measurements were performed with a Rigaku Geiger Flex D/max RB X-ray diffractometer with Cu Kα radiation at a heating rate of 1°/min.

Investigation of the dynamic curing behaviors of the BZ–MMT system by DSC

Curing studies in the dynamic mode were carried out with a PerkinElmer 2C differential scanning calorimeter operating in a nitrogen atmosphere. The DSC instrument was calibrated by indium standards, and a-Al_2O_3 was used as the reference material.

About 3 mg of BZ–MMT was placed in a sample cell. Dynamic DSC tests were run at 2.5, 5, 10, and 20°C/min. About 3 mg of BZ was placed in a sample cell, and dynamic DSC tests were run at 20°C/min. The reaction was considered complete when the rate curve leveled off to a baseline. The kinetic parameters from the single-heating-rate method were then calculated with PerkinElmer DSC kinetics analysis software.

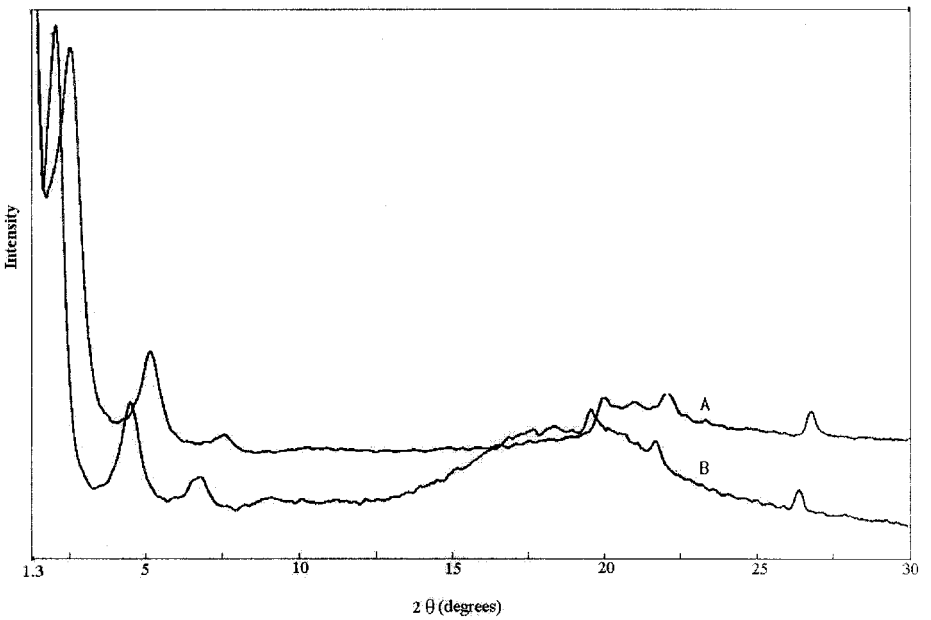

Figure 1 XRD patterns of (A) O-MMT and (B) PBZ–MMT nanocomposites.

RESULTS AND DISCUSSION

Structural characterization of the PBZ–MMT nanocomposites

For natural MMT, its hydrophilicity results in poor compatibility with organic materials, so it is difficult for the layered silicate to intercalate and disperse uniformly in a polymer matrix. As MMT has an excess negative charge, it can be combined with organophilic alkylammonium ions to yield O-MMT, and this allows its homogeneous dispersion in the polymer matrix. Specifically, the O-MMT used in this study was washed with water and ethanol for the removal of excess quaternary ammonium salt. O-MMT displayed an interlayer spacing of 3.4 nm.

Figure 1 presents XRD curves of O-MMT and PBZ–MMT nanocomposites in the region from 1.3 to 30, and Table I shows the 001 lattice spacing of O-MMT in three different systems. In comparison with O-MMT, the PBZ–MMT nanocomposites had a new set of peaks. As previously reported,[12] the diffraction peaks in the range of 2θ = 3–9 were assigned to the 001 lattice spacing, which corresponded to the interlayer spacing of O-MMT. Either an intercalated nanocomposite or an immiscible system can be determined by the change in the interlayer spacing. Figure 1 shows that the diffractions of the 001 lattice spacing of O-MMT in the nanocomposites shifted to lower angles in comparison with that of O-MMT, and this revealed that the basal spacing increased from 3.4 to 4.2 nm. Therefore, the XRD analysis suggested that chains of PBZ were successfully inserted into the interlayers of O-MMT to form intercalated nanocomposites because of the good compatibility between PBZ and O-MMT. In addition, it can be seen in Table I that the 001 lattice spacing in the BZ–MMT system was almost the same as that in the PBZ–MMT system, and this shows that the monomer of PBZ was intercalated into the O-MMT gallery at first and then polymerized within the O-MMT galleries. Therefore, from the analysis of the nature of PBZ/O-MMT by XRD, it was proven that PBZ could intercalate into the gallery of O-MMT to form an intercalated nanocomposite.

TABLE I
001 Lattice Spacing in Three Different Systems

	O-MMT	BZ–MMT	PBZ–MMT
001 Lattice spacing (nm)	3.5	4.1	4.2

Comparison of the dynamic curing behaviors of the BZ–MMT and BZ systems

The dynamic exothermal curves of the two systems at a heating rate of 20°C/min are shown in Figure 2. One exothermal peak could be observed for each curing system. However, for the BZ system, there was a sharp exothermal peak in the range of the curing temperature, whereas for the BZ–MMT system, the exothermal peak was smooth and broad, with a shift of the exothermal peak to a lower temperature with respect to the BZ system. Also, the polymerization process in the BZ system occurred much more rapidly than that in the BZ–MMT system. The variation of the reaction rate in the BZ–MMT system was small in comparison with that in the BZ system. The ratio of the maximum reaction rate to the minimum was 7 in the BZ–MMT system. However, the ratio was 196 in the BZ system.

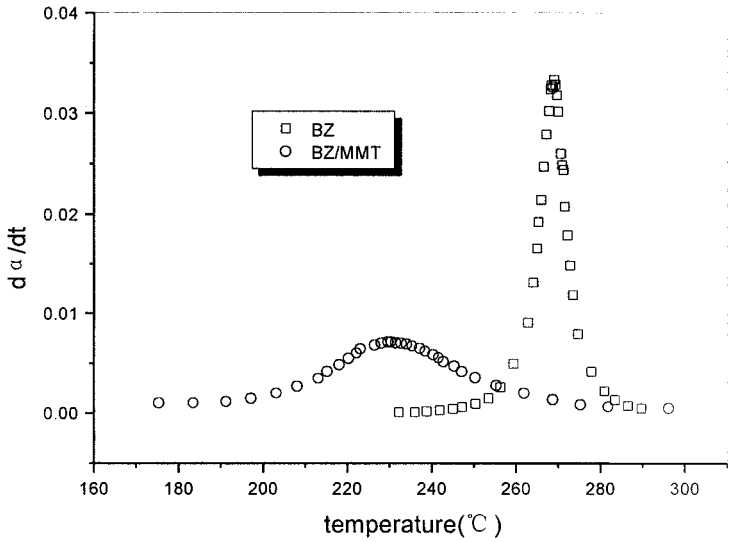

Figure 2 Dynamic exothermal curves of two systems at a heating rate of 20°C/min.

Consequently, the change in the curing rate in the BZ–MMT system was not great over a wider range of curing temperatures. This also means that the curing reaction proceeded relatively smoothly, whereas the curing reaction in the BZ system was delayed to a higher temperature. When the reaction was initiated, the polymerization occurred rapidly, the curing rate changed greatly, and the curing reaction was finally completed in a narrow range of higher curing temperatures; this is characteristic of a thermal curing reaction.[25] The different features in the curing rates of the two curing systems indicated that there were different curing mechanisms in the BZ–MMT system and the BZ system. Therefore, it is important to research the curing kinetic of the BZ–MMT system, which is the basis for designing an optimum curing procedure.

Investigation of the nonisothermal kinetics of the BZ–MMT system by DSC

DSC is an attractive technique because it can provide detailed knowledge of the cure mechanism and the preferred temperature during the formation of three-dimensional networks in materials. In addition, it is simple to use, data are obtained quickly, and only small quantities of resin are required.[28] DSC has been employed widely to elucidate key cure process parameters, such as the extent and rate of chemical conversion and the glass-transition temperature, in both isothermal and dynamic DSC experiments, under the assumption that the heat evolved during cure is proportional to the extent of the reaction.[29]

Figure 3 shows the results for DSC exotherm curves

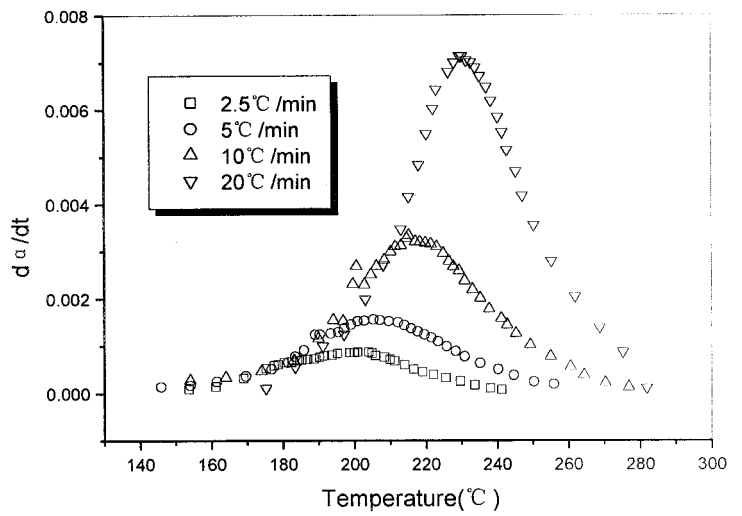

Figure 3 Dynamic DSC spectra at different scanning rates in the BZ/MMT system.

TABLE II
Characteristic Temperatures at Different Scan Rates

ϕ (°C/min)	T_i (°C)	T_p (°C)	T_f (°C)	ΔT (°C)	ΔH (J/g)
2.5	144.99	196.32	243.75	98.76	207.44
5	137.81	204.37	267.81	130	284.80
10	144.05	217.18	282.18	138.13	297.69
20	167.80	230.31	296.87	129.07	320.12

ΔT = range of curing temperature.

at 2.5, 5, 10, and 20°C/min. Table II tabulates the characteristic curing parameters obtained from Figure 3. In Table II, it can be seen that the onset-of-curing temperature [or isoconversion temperature (T_i)], the peak-of-curing temperature [or peak exotherm temperature (T_p)], and the termination-of-curing temperature (T_f) all increased with an increase in the heating rate. The wider the curing temperature range was, the higher the heating rate was. The observed total reaction heat, ΔH, was not constant, and this shows that its value increased as the heating rate increased from 2.5 to 20°C/min. These exotherms were investigated with nonisothermal methods, which included the single-heating-rate and multiple-heating-rate methods, to obtain the activation energy (E) value and other related parameters.

DSC single-heating method

The DSC single-heating method[30,31] measures the curing process from only a single constant-heating-rate cycle. The direct derivation of the kinetic parameters associated with the curing reaction from the single-heating method is based on an analysis of the data with the methods of Rogers and Smith and Piloyan et al.[30,31] The overall rate of the curing reaction is always expressed as follows, with nth-order kinetics assumed:

$$\frac{da}{dt} = k(1-a)^n \tag{1}$$

where a is the fraction reacted, that is, the fraction of the total possible enthalpy; k is the overall rate constant; and n is the overall order of the curing reaction. k is usually assumed to have an Arrhenius-type temperature. Therefore, eq. (1) can be transformed as follows:

$$\frac{da}{dt} = A\exp\left(-\frac{E}{RT}\right)(1-a)^n \tag{2}$$

By taking the logarithm on both sides, we can modify eq. (2) as follows:

$$\ln\frac{da}{dt} = \ln A - \frac{E}{RT} + n\ln(1-a) \tag{3}$$

TABLE III
Results of the Curing Reaction Dynamic Data

ϕ (°C/min)	E (kJ/mol)	n
2.5	110.79	1.42
5	99.68	1.28
10	102.69	1.21
20	108.08	1.31

Differentiating, integrating, and finally rearranging eq. (3) yield the Freeman–Carroll relation:

$$\frac{\Delta\left(\ln\frac{da}{dt}\right)}{\Delta\ln(1-a)} = -\frac{E}{R}\left[\frac{\Delta\frac{1}{T}}{\Delta\ln(1-a)}\right] + n \tag{4}$$

The data provided by DSC, plotted according to eq. (4), yield a straight line of slope $-(E/R)$ and intercept n (where R is the universal gas constant). The data treatment permits the simultaneous evaluation of E and n.

It is evident that the single-heating method is based on the nth-order kinetic reaction, which can probably limit the reliability of the system as many systems are in fact not of the nth-order type, although the advantage is that it can be convenient to provide extensive information from only a single dynamic scan.[28] Therefore, the method can easily estimate the parameters in the kinetics of a reaction approximately to determine the relationship of the parameters and heating rates to gain a general idea of the cure mechanism.

The dynamic curing behaviors for the BZ–MMT system were investigated by the single-heating method. Table III shows the results obtained by the single-heating method, including the kinetic parameters from different constant heating rates. The overall value of E was 99.68–110.79 kJ/mol, and the average of the overall value of E was about 105.31 kJ/mol. n was in the narrow region of 1.21–1.42, and its average was about 1.31. Therefore, it is thought that the overall values of E and n were not very sensitive to the heating rate. In other words, this means that the changes in E and n were not large as the heating rate was increased.

DSC multiple-heating-rate methods

The multiple-heating-rate methods, the other nonisothermal methods, are isoconversion methods; that is,

TABLE IV
DSC α_p's at Different Heating Rates

ϕ (°C/min)	α_p
2.5	48.02
5	48.65
10	49.78
20	49.03

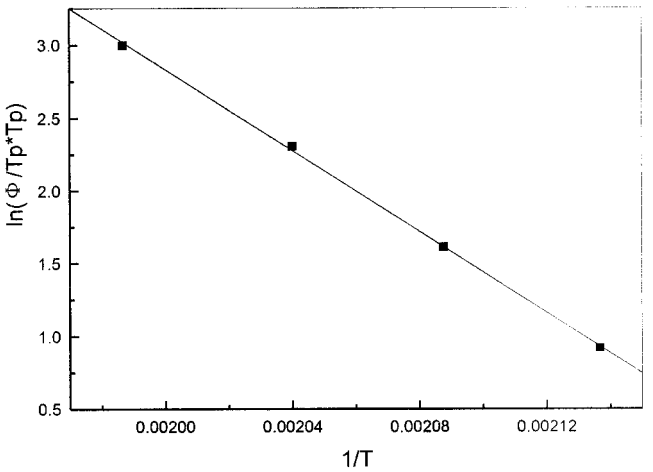

Figure 4 Plots for the determination of E of the curing reaction by the Kissinger method.

they assume that the conversion value α_p is constant at T_p in a DSC analysis and is independent of the heating rate.[32] This makes them equally effective for both nth-order and autocatalytic reactions.[32]

Kissinger method[33,34]

The nonisothermal kinetics for the BZ–MMT system were investigated by the Kissinger method, which is one of the multiple methods. It uses the following relationship: for thermoset curing, the extent of the reaction at the peak exotherm is constant and independent of the heating rate. E can be obtained as follows:

$$\frac{d[\ln(\phi/T_p^2)]}{d(1/T_p)} = -\frac{E}{R} \tag{5}$$

where Φ is the heating rate. It is simplistic to assume a single reaction occurring during the curing process, given the complexity of the reaction.[33] Therefore, the value of E in eq. (5) is an overall value representing all complex reactions that occur during curing.[33]

Table IV tabulates the results obtained for the conversion at the peak exotherm for different heating rates. It is evident that the conversion values obtained were very close in value, confirming that for the system tested, the assumption that the conversion was independent of the heating rate was valid.

On the basis of eq. 5, E was obtained by the plotting of $\ln(\Phi/T_p^2)$ against $1/T_p$. This is shown in Figure 4, which displays the experimental data obtained for the BZ–MMT system tested. A linear relationship was obtained, confirming the validity of the proposed model given in the equation. E was calculated from the slope, which yielded a value of 115 kJ/mol, which was slightly higher than that obtained from the single-heating method.

Ozawa method[35]

The Ozawa method, another multiple-heating method, yields a simple relationship for E, Φ, and T_i:

$$E = \frac{-R}{1.052}\frac{\Delta \ln \phi}{\Delta(1/T_i)} \tag{6}$$

The advantage here is that E can be measured over the entire course of the reaction. Therefore, the nonisothermal curing kinetics for the BZ–MMT system were investigated with the Ozawa method.

Figure 5 plots the conversion percentage against the dynamic cure temperature, for the various heating rates shown, according to the results obtained from the DSC curves shown in Figure 3. From Figure 5, it is seen that at the same conversion value, T_i was higher when the test heating rate was increased. Based on eq. 6, the plot of ln Φ against $1/T_i$ enabled the calculation

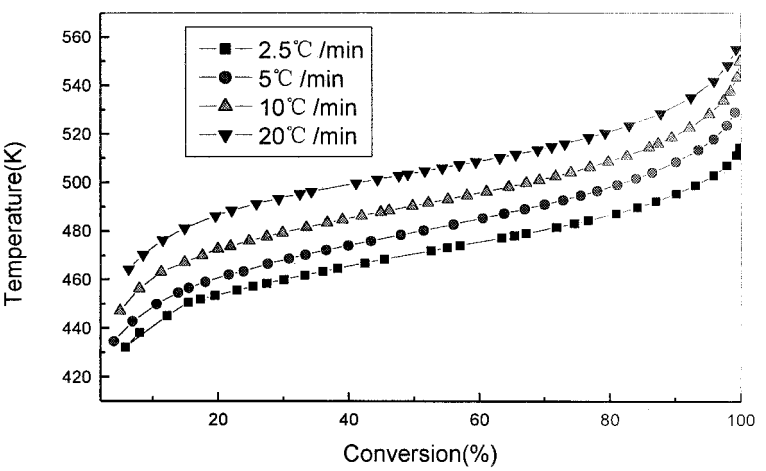

Figure 5 Plots of the DSC values of T_i at different heating rates.

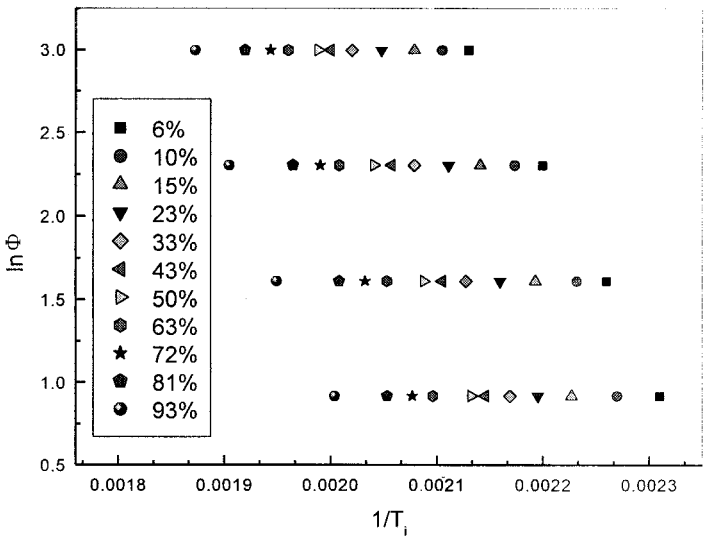

Figure 6 Plots of ln Φ against $1/T_i$ at different conversions for the calculation of E.

of E at any conversion by the Ozawa method, and this is shown in Figure 6 for conversions from 6 to 93%.

Figure 6 plots the values of E calculated by the Ozawa method for different values of the conversion, showing that E gradually increased with the extent of cure. This might have been due to the reduction in the mobility of the reactive groups of the partially cured BZ. The value of E was about constant in the interval $15\% < \alpha < 72\%$. E was found to be 120 kJ/mol, which was slightly higher than those values obtained by the Kissinger method and the single-heating method.

CONCLUSIONS

The intercalated structure of the PBZ–MMT nanocomposites was characterized with XRD. An accurate model of the cure kinetics of the BZ–MMT system was elucidated with three different nonisothermal DSC methods. The results indicated that both the Kissinger and Ozawa methods for calculating E gave fairly close results of 115 and 120 kJ/mol, respectively. The single method, based on the autocatalytic model, calculated the total order of reaction to be about 1.31.

References

1. Kawasumi, M.; Hasegawa, N.; Kato, M.; Usuki, A.; Okada, A. Macromolecules 1997, 30, 6333.
2. Huang, X.; Lewis, S.; Brittain, W. J. Macromolecules 2000, 33, 2000.
3. Chin, I.; Albrecht, T. T.; Kim, H.; Russell, T. P.; Wang, J. Polymer 2001, 42, 5947.
4. Usuki, A.; Kawasumi, M.; Kojima, Y.; Okada, A.; Kurauchi, T.; Kamigaito, O. J Mater Res 1993, 8, 1179.
5. Vaia, R. A.; Jandt, K. D.; Kramer, E. J.; Giannelis, E. P. Macromolecules 1995, 28, 8080.
6. Messersmith, P. B.; Giannelis, E. P. J Polym Sci Part A: Polym Chem 1995, 33, 1047.
7. Varia, R. A.; Sauer, B. B.; Tse, O. K.; Giannelis, E. P. J Polym Sci Part B: Polym Phys 1997, 35, 59.
8. Zhu, Z. K.; Yin, J. J Appl Polym Sci 1999, 73, 2063.
9. Yang, Y.; Zhu, Z.; Yin, J.; Wang, X.; Qi, Z. Polymer 1999, 40, 4407.
10. Wang, Z.; Pinnavia, T. J. Chem Mater 1999, 11, 1942.
11. Wang, M. S.; Pinnavia, T. J. Chem Mater 1994, 6, 2216.
12. Messersmith, P. B.; Giannelis, E. P. Chem Mater 1994, 6, 1719.
13. Langley, N. R.; Mbah, G. C.; Freeman, H. A.; Huang, H.; Siochi, E. J.; Ward, T.; Wilkes, G. J. Colloid Interface Sci 1991, 143, 309.
14. Wang, Z.; Pinnavia, T. J. Chem Mater 1998, 10, 3769.
15. Agag, T.; Takeichi, T. Polymer 2000, 41, 7083.
16. Ishida, H. Compos Transp Ind, Proc ACUN-2: 2nd Int Compos Conf, 2000, 2, 458.
17. Ishida, H. U.S. Pat. 6,323,270 (2001).
18. Phiriyawirut, P.; Magaraphan, R.; Ishida, H. Mater Res Innovations 2001, 4, 187.
19. Takeichi, T.; Zeidam, R.; Agag, T. Polymer 2002, 43, 45.
20. Ishida, H.; Low, H. Y. Macromolecules 1997, 30, 1099.
21. Ishida, H.; Rodriguez, Y. Polym Mater Sci Eng 1995, 73, 498.
22. Ishida, H.; Rodriguez, Y. J Appl Polym Sci 1995, 58, 1751.
23. Low, H. Y.; Ishida, H. Polymer 1999, 40, 4365.
24. Wang, Y. X.; Ishida, H. Polymer 1999, 40, 4563.
25. Rimdusit, S.; Ishida, H. Polymer 2000, 41, 7941.
26. Shi, Z. X. Ph.D. Dissertation, Beijing University of Chemical Technology, 2000.
27. Kojima, T.; Usuki, A.; Kawasumi, M.; Okada, A.; Kurauchi, J.; Kamigaito, O. J Appl Polym Sci 1993, 49, 1259.
28. Boey, F. Y. C.; Qiang, W. Polymer 2000, 41, 2081.
29. Khanna, U.; Chanda, M. J Appl Polym Sci 1993, 49, 319.
30. Patel, R. D.; Patel, R. G.; Patel, V. S. Br Polym J 1987, 19, 37.
31. Shah, P. P.; Parsania, P. H.; Patel, S. R. Br Polym J 1985, 17, 354.
32. Prime, P. B. Polym Eng Sci 1973, 13, 365.
33. Duffy, J. V.; Hui, E.; Hartmann, B. J Appl Polym Sci 1987, 33, 2959.
34. Kissinger, H. E. Anal Chem 1957, 29, 1702.
35. Horie, K.; Hiura, H.; Souvada, M.; Mita, I.; Kambe, H. J Polym Sci Polym Chem 1970, 8, 1357.